

Specific-heat spectroscopy and dielectric susceptibility measurements of salol at the glass transition

Paul K. Dixon*

The James Franck Institute and The Department of Physics, The University of Chicago, Chicago, Illinois 60637

(Received 18 June 1990)

We compare specific-heat-spectroscopy and dielectric susceptibility measurements of salol (phenyl salicylate) near the glass transition. The specific-heat-spectroscopy measurements cover 5 decades in frequency; the dielectric susceptibility measurements cover 13 decades. Over their common range, both probes measure the same characteristic relaxation time. In contrast to the viscosity measurements of salol reported in the literature, the characteristic relaxation time measured by these techniques shows non-Arrhenius behavior near T_g . The Vogel-Fulcher divergence temperature is consistent with the Kauzmann temperature. As is seen in other glass formers, the relaxation widths broaden rapidly with decreasing temperature.

I. INTRODUCTION

As a practical matter, the transition from a supercooled liquid to a glass is the result of the liquid slowing down and falling out of equilibrium as it is cooled. The temperature at which the characteristic relaxation time τ reaches $\sim 10^4$ sec is commonly designated the glass-transition temperature T_g . A fundamental question arises: Is the observed dynamic slowing down in the liquid being driven by an underlying thermodynamic phase transition or is it simply a kinetic effect? At present, there is no clear answer to this question; unlike most simple phase transitions, the glass transition does not have a clear order parameter with a simple symmetry.

An observation in favor of the phase-transition picture of the glass transition was made by Kauzmann;¹ he noted that for most glass formers, an extrapolation of the supercooled liquid entropy below T_g crosses the associated crystalline value at a nonzero temperature T_K . This implies that the equilibrium liquid must change in some way at, or above, T_K to avoid this paradoxical situation. If the characteristic relaxation time τ of the liquid were not to diverge above T_K , then such an entropy crossing would occur. For many glass-forming liquids,² τ can be fit with a Vogel-Fulcher form $\tau = \tau_0 \exp[A/(T - T_0)]$, with $T_0 \approx T_K$. This suggests that T_K plays a role in both the statics and dynamics of the glass transition.

In the entropic theories of the glass transition,³ T_K is identified as the equilibrium glass-transition temperature. The basic premise of these theories is that the relaxation of a supercooled liquid is due to the activated exploration of the possible particle configurations available on the potential-energy hypersurface. The configurational entropy $\Delta S = S(\text{liquid}) - S(\text{crystal})$ is a measure of the number of configurations available at a given temperature. By assumption, $\Delta S(T_K) = 0$, meaning that the number of potential-energy minima available to the system as $T \rightarrow T_K$ approaches a number of order unity; as a result,

the time scale required for the system to relax diverges.

In the "strong" to "fragile" classification scheme proposed by Angell,² it has been found that this picture of the glass transition is consistent with the observed dynamics for the strong and intermediate glass formers. Unfortunately, this picture appears to break down at the fragile end of the spectrum. Viscosity measurements^{4,5} on a number of fragile glass formers indicate that the shear relaxation time τ_s is diverging in an Arrhenius fashion, $\tau_s = \tau_{s0} \exp(A_s/T)$, near T_g . Salol (phenyl salicylate) is one of the fragile glass formers for which this is the case. The fragile end of the spectrum is where the entropy crisis is the most dramatic, with T_K typically 30–60 K below T_g . Since we can get closer to T_K in these liquids than in the strong liquids, we expect that the equilibrium dynamics near T_g in these cases will more clearly reflect the underlying phase transition if it exists. The reported⁴ Arrhenius behavior indicates that there may be no phase transition at all; the glass transition may be a purely kinetic effect.

We have tried to resolve this issue by studying the equilibrium dynamics near T_g in salol using specific-heat spectroscopy^{6–14} (SHS) and dielectric susceptibility.¹⁵ The entropy crisis at T_K is due to the fact that the specific heat c_p of the liquid is higher than that of the corresponding crystal; this extra specific heat is the contribution of the slowly relaxing liquidlike degrees of freedom. Clearly, it is more appropriate to measure the relaxation in c_p directly; SHS was designed to do precisely this.

Dielectric susceptibility has the advantage that it can be used to obtain exceptionally precise measurements of the relaxation over a large bandwidth; this makes it a good complement to SHS, which is limited in both. The extremely large bandwidth (13 decades) that was covered in dielectric susceptibility allows one to track the evolution of the primary relaxation from the simple liquid behavior above the melting point all the way down to T_g . Since both of these techniques are frequency-dependent susceptibilities, we can obtain not only the behavior of

their mean relaxation times, as in a viscosity measurement, but the entire form of the relaxation.

II. TECHNIQUE

A. Specific-heat spectroscopy

SHS measures the frequency-dependent specific heat $c_p(\nu)$. It is the linear response of the enthalpy of a system in equilibrium to a small temperature oscillation at a frequency ν ; in the limit $\nu=0$, it is the conventional specific heat. In practice, the basic technique measures the product of the specific heat and thermal conductivity $c_p\kappa(\nu)$. In a previous experiment¹⁰ we showed that c_p is the dynamic variable; κ shows no dispersion through the glass transition. For a thorough review of the technique, we refer the reader to Refs. 8–10.

As in previous experiments,^{9,10} we made measurements with three heaters of differing width to cover the range 20 mHz $< \nu < 5$ kHz. The combination of the limited signal to noise of this technique and the need to maintain equilibrium throughout the measurement required us to use very slow cooling rates ($\sim 1-3$ K/h) in the neighborhood of T_g . This led to a very high probability of crystallization of the liquid. This, in turn, resulted in the destruction of a number of the heaters because the growing crystal pulled the heaters off the substrate. The crystallization invariably destroyed the low-band heater first; consequently, we were unable to obtain high-precision low-band heater data above 100 mHz. As a result, we do not have the base line necessary to separate out the contributions of c_p and κ to the dynamics as we did in a previous measurement.¹⁰

B. Dielectric susceptibility

Dielectric susceptibility measures the frequency-dependent dielectric response $\epsilon(\nu)$. For polar liquids like salol, it allows us to measure the relaxation of the molecular component of the polarization of the liquid. For a review of dielectric susceptibility measurements, we refer the reader to Refs. 16–18.

The data were taken by a variety of means. Over the range 1 mHz $< \nu < 10$ MHz, we used a multiplate parallel-plate capacitor (dry capacitance ~ 100 pF) totally immersed in the liquid in a temperature-controlled can; this resulted in a “wet” capacitance of ~ 1 nF ($\epsilon \sim 10$ for salol). From 1 mHz to 10 kHz, we used a Hewlett-Packard 3325A synthesizer, a Keithley 427 current amplifier, and a Digital lock in¹⁹ of our own design in a conventional virtual ground impedance measurement configuration. From 10 kHz to 10 MHz, we used a Hewlett-Packard 4275A four-probe impedance analyzer.

Temperature control and measurement for the configuration above was by way of calibrated platinum resistance thermometry. All of the data was taken while ramping at a constant rate anywhere from 1 to 0.05 K/min, depending on the measuring frequencies and temperature range. We measured temperature using two thermometers: one embedded in the temperature control

can and the other embedded in the capacitor itself. This allowed us to determine and correct for thermal gradients due to a variety of effects including the ramping. More importantly, it gave us a method independent of the dielectric measurement to determine whether or not the liquid was in equilibrium. The temperature difference between the two thermometers includes a term proportional to c_p/κ of the intervening liquid. When cooling through the temperature at which the liquid falls out of equilibrium for a given cooling rate, we observed a drop in the temperature difference between the two thermometers, analogous to the drop in c_p measured by differential scanning calorimetry.²⁰ Equivalently, for heating, we observed the corresponding jump in the temperature difference. This allowed us to accurately determine our equilibrium temperature range for any given run; all of the data we present were measured in equilibrium. We controlled temperature to a precision better than 10 mK; we estimate that our temperature data are accurate within a global shift of 0.5 K.

Over the frequency range 50 MHz $< \nu < 20$ GHz, the data were taken in both transmission and reflection with a 50- Ω coaxial transmission line and a Hewlett-Packard 8510B network analyzer. A known length of the transmission line was filled with the liquid. To maintain a filled cell over a broad temperature range, the liquid was allowed to flow between the transmission line and fluid reservoirs through small pinholes. We designed the cell and analyzed the data using techniques discussed in the relevant Hewlett-Packard 8510 network analyzer application notes.²¹ The coaxial liquid cell was contained in a temperature-control support structure. This data was taken while ramping temperature at a constant rate in a manner similar to the technique outlined above.

C. Sample preparation

We obtained our salol samples from the Aldrich Chemical Company in crystalline form; the supplier assay of our sample (lot No. 04129LT) claims a purity greater than 99%. Although salol appears to be relatively immiscible with water, we took the precaution of always maintaining our liquid samples in a dry-nitrogen atmosphere. Before placing the liquid in our various measuring cells, we kept it in a vacuum oven at $\sim 60^\circ\text{C}$ ($T_m = 44-46^\circ\text{C}$) for at least 24 h. We discovered that prolonged exposure to excessive temperature ($> 80^\circ\text{C}$) or bright light led to a brownish discoloration of the liquid. This discoloration was accelerated in the presence of copper and brass; consequently, all of our measurement cells were made out of aluminum, which showed no such effect.

III. EXPERIMENTAL RESULTS AND DISCUSSION

A. Specific-heat spectroscopy data

We performed SHS measurements on supercooled salol in equilibrium above T_g . In Fig. 1 we show the real ($c_p\kappa'$) and imaginary ($c_p\kappa''$) parts of $c_p\kappa(\nu)$ versus $\log_{10}(\nu)$ at three temperatures. As is apparent in the

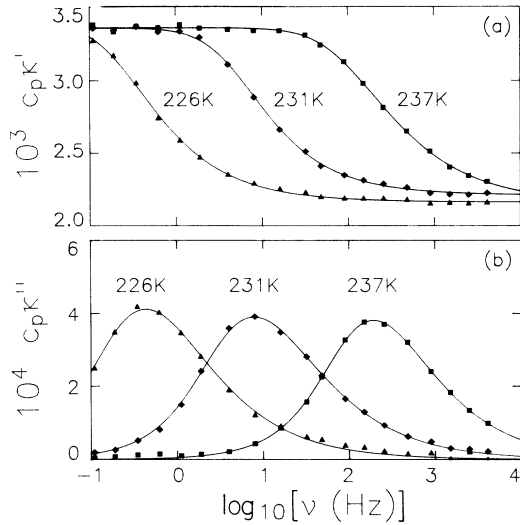


FIG. 1. (a) Real $c_p\kappa'$ and (b) imaginary $c_p\kappa''$ parts of $c_p\kappa$ ($\text{J}^2/\text{K}^2\text{cm}^4\text{s}$) vs $\log_{10}[\nu$ (Hz)] at the labeled temperatures. The curves are best fits to the data using the stretched-exponential form.

figure, the relaxing component of $c_p\kappa$ is asymmetrical and the average relaxation time grows with decreasing T . These features are common to all equilibrium susceptibility measurements at the glass transition.

The curves drawn through the $c_p\kappa''$ data are best fits using the Kohlrausch-Williams-Watts (stretched-exponential) form: the Fourier transform of $-d\{\Delta(c_p\kappa)\exp[-(2\pi\nu_{\text{SE}}t)^\beta]\}/dt$, where $\Delta(c_p\kappa)=[c_p\kappa(\nu=0)-c_p\kappa(\nu=\infty)]$. The curves drawn through the $c_p\kappa'$ data are obtained by using the parameter values obtained from the $c_p\kappa''$ data and allowing $c_p\kappa(\nu=\infty)$ to be the only additional fitting parameter. The quality of the $c_p\kappa'$ fits confirms that the data obey the Kramers-Kronig relations. We also tried the Davidson-Cole form¹⁶ $c_p\kappa(\nu)=c_p\kappa(\nu=\infty)+\Delta(c_p\kappa)/(1+i\nu/\nu_{\text{DC}})^\delta$, but found the stretched-exponential form superior.

B. Dielectric susceptibility data

We also present the dielectric susceptibility measurements for salol taken from Ref. 15. The data cover the range $1\text{ mHz} < \nu < 20\text{ GHz}$. In Fig. 2 we show the real (ϵ') and imaginary (ϵ'') parts of $\epsilon(\nu)$ versus $\log_{10}(\nu)$ at the labeled temperatures. These data show the same qualitative features evident in the $c_p\kappa$ data of Fig. 1.

As was the case with the $c_p\kappa$ data, the curves drawn through the data are best fits using the stretched-exponential form. Again, we also tried the Davidson-Cole form,¹⁶ but found the stretched-exponential form superior. These data also obey the Kramers-Kronig relations as expected. In this case, the measurement is precise enough to determine that neither form fits the data well in the high-frequency tail. Even though the stretched-exponential fits are clearly inadequate, they still measure adequately the peak position, width, and general asymmetry of the relaxation.

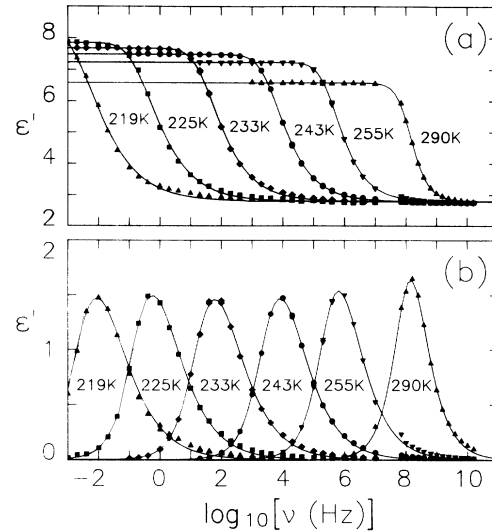


FIG. 2. (a) Real ϵ' and (b) imaginary ϵ'' parts of ϵ vs $\log_{10}[\nu$ (Hz)] at the labeled temperatures. The curves are best fits to the data using the stretched-exponential form. Note that the fits are deficient in the high-frequency tails.

The inadequacy of these empirical forms to fit the dielectric data is not unique to salol. This property was found for all of the supercooled liquids measured in Ref. 15. The fact that the stretched-exponential form is adequate to fit the SHS data should not be misinterpreted as a confirmation of the relaxation form in that case. Our SHS data do not have the precision necessary to observe deviations on the order of those observable in the dielectric susceptibility measurements. A close examination of the data suggests that it is very possible that the relaxation shape that we see in the dielectric susceptibility data will show up in future SHS measurements with improved precision.

Since we know that the fitting forms are inadequate, we choose to parametrize the data in a fashion divorced from any particular form. We have used the peak relaxation frequency ν_p and the normalized width w ; w is the full width at half maximum (W) divided by the Debye width ($W_D=1.142$ decades): $w \equiv W/W_D$. The stretched-exponential fitting parameters ν_{SE} and β can be obtained from the peak position and width. To a very good approximation over the range $0.4 < w^{-1} < 1.0$, we find that

$$\log_{10}(\nu_{\text{SE}}) = \log_{10}(\nu_p) + 0.272(1 - w^{-1}),$$

and

$$(1 - \beta) = 1.047(1 - w^{-1}).$$

C. Peak relaxation frequencies, low T

In Fig. 3(a) we show the logarithm of the peak relaxation frequency $\log_{10}(\nu_p)$ versus $1/T$ for both techniques. To compare the relaxation times obtained from the two techniques, we must take into account the different thermodynamic basis of the two measurements.²² The dielec-

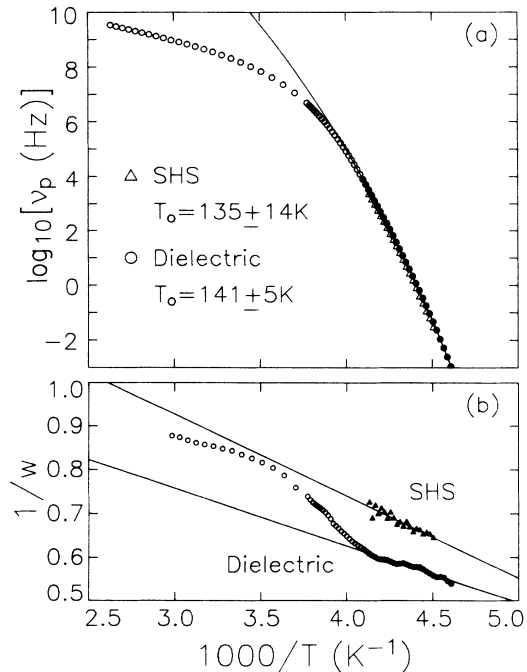


FIG. 3. (a) Logarithm of the peak relaxation frequency $\log_{10}[\nu_p \text{ (Hz)}]$ vs $1000/T \text{ (K}^{-1}\text{)}$ for SHS (Δ) and dielectric susceptibility (\circ). The curve is a best fit to the dielectric data over the range $1 \text{ mHz} < \nu_p < 10 \text{ kHz}$ using the Vogel-Fulcher form; the data points that were fitted are designated by solid circles. The Vogel-Fulcher fitting parameters for both sets of data are listed in Table I. (b) Normalized inverse width $w^{-1} = W_D/W$ vs $1000/T \text{ (K}^{-1}\text{)}$ for SHS (Δ) and dielectric susceptibility (\circ). The curves are fits to the data using the form $w^{-1} = a + b/T$; the dielectric data were fit over the range $1 \text{ mHz} < \nu_p < 10 \text{ kHz}$; again, the fitted data points are designated by solid circles.

tric data, which are adiabatic, have been corrected by the factor $\nu_{\text{iso}} = [c_p(\nu = \infty)/c_p(\nu = 0)]\nu_{\text{adb}}$ to compare them to the SHS data, which are isothermal. The values of $c_p(\nu = \infty)$ and $c_p(\nu = 0)$ were obtained from Ref. 4; $c_p(\nu = \infty)/c_p(\nu = 0) \sim 0.7$ and is slowly varying. The “elbow” region where the relaxations of fragile liquids cross over from their high- to low- T regime is clearly evident in the dielectric data. Over their common range, the two techniques appear to measure the same characteristic relaxation frequency. More important, the relaxations show no sign of crossing over to Arrhenius behavior near T_g as has been seen in viscosity⁴ measurements in this range. Let us first discuss the low-temperature behavior of these relaxations where we have data from both techniques and then broaden the scope of our discussion to the entire range covered by the dielectric data.

The curve in Fig. 3(a) is a Vogel-Fulcher fit $\nu_p = \nu_f \exp[-A_f/(T - T_0)]$ to the dielectric data in the low- T regime (1 mHz to 10 kHz) with $T_0 = 141 \pm 5 \text{ K}$; a fit to the SHS data gives $T_0 = 135 \pm 14 \text{ K}$. The complete fitting parameters for both measurements are listed in Table I. Using the specific-heat data for both liquid and crystalline salol obtained from Ref. 4 and the heat-of-fusion data from Ref. 23, we calculate $T_K = 157 \pm 12 \text{ K}$ for salol. The

TABLE I. Fitting parameters for the data in Fig. 3(a) using the Vogel-Fulcher form: $\nu_p = \nu_f \exp[-A_f/(T - T_0)]$. The dielectric data have been fit over the range $1 \text{ mHz} < \nu_p < 10 \text{ kHz}$.

Technique	$T_0 \text{ (K)}$	$A_f \text{ (K)}$	$\log_{10}[\nu_f \text{ (Hz)}]$
SHS	135 ± 14	5220 ± 350	24.5 ± 1.4
Dielectric	141 ± 5	4633 ± 120	23.3 ± 0.5

T_0 and T_K values are within error, but these data show a feature seen in many glass formers;² the measured values of T_0 are typically $\sim 5\text{--}20 \text{ K}$ below T_K . This common discrepancy is not understood.

Considering that the dielectric data in Fig. 3(a) cannot be fit with a single Vogel-Fulcher form over the entire range, the following question arises. Is the observed curvature in the low- T regime just an effect of the crossover from some high- T behavior to a low- T Arrhenius behavior with a high activation energy? In other words, does the measured $T_0 \rightarrow 0$ as $T \rightarrow 0$? We have tried to answer this question by measuring T_0 locally using a three-decade fit and sliding the fitting window through the data to observe the trend in T_0 as T is lowered. In Fig. 4 we plot the T_0 measured for the three-decade fits versus the logarithm of the low-frequency cutoff of the fits $\log_{10}(\nu_{\text{low}})$. For example, the dielectric T_0 value plotted for $\log_{10}(\nu_{\text{low}}) = 1$ was obtained by fitting the dielectric data in Fig. 3(a) over the range $10 \text{ Hz} < \nu_p < 10 \text{ kHz}$. It is clear from Fig. 4 that values of T_0 obtained from the data below 10 kHz in both techniques appear stable. There is no evidence in our data that the relaxations are crossing over into Arrhenius behavior. This leads us to two possible conclusions. Either the shear relaxation is decoupling from the relaxation mechanism measured with SHS and dielectric susceptibility, or the viscosity measurements on salol are inaccurate. We believe it is

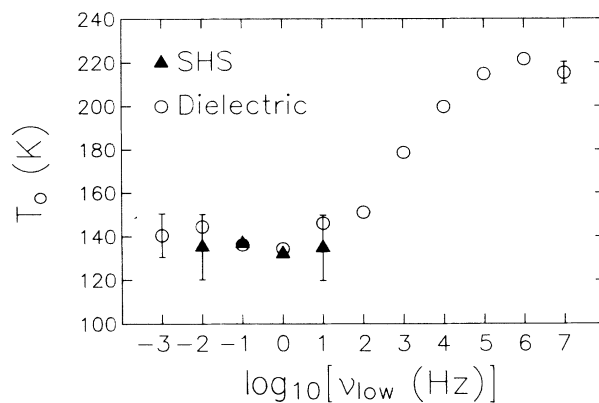


FIG. 4. Vogel-Fulcher divergence temperature $T_0 \text{ (K)}$ obtained from three-decade fits to the data in Fig. 3(a) vs the low-frequency cutoff of the fits, $\log_{10}[\nu_{\text{low}} \text{ (Hz)}]$. The dielectric data (\circ) show a clear crossover in T_0 from the high- T range to the low- T range; the SHS (Δ) data do not extend to high enough frequency to observe this. Note that the values of T_0 obtained from fits to the data with $\nu_p < 10 \text{ kHz}$ appear stable.

the latter case; a close inspection of the viscosity data⁴ reveals that the scatter in those data are too large to distinguish a Vogel-Fulcher behavior consistent with our data from an Arrhenius form.

D. Relaxation widths

In Fig. 3(b) we plot the inverse of the normalized width w^{-1} vs $1/T$ for both measurements. Both techniques show strong temperature dependence of the width. In particular, the dielectric data show a rapid broadening in the same temperature range where the peak relaxation frequency data steepens; the behavior of the width and peak position appears to be correlated. The relationship between the dielectric and SHS values of the width is not understood and does not show any clear correlation from one liquid to another.^{7,11,15} It should not be surprising that the values of w are different for the two techniques, considering that SHS couples to relaxing modes in an unbiased manner, whereas dielectric susceptibility couples in proportion to a mode's dipole moment.

The temperature dependence of these SHS width data is similar to the behavior observed in a previous measurement of the fragile glass former *o*-terphenyl.¹⁰ As was the case with *o*-terphenyl, fitting these SHS w^{-1} data with a form linear in $1/T$ [shown in Fig. 3(b)] gives an extrapolation to $w^{-1}=0$ at $T=130\pm 15$ K, which is very close to the divergence temperature $T_0=135\pm 14$ K obtained from the peak frequency data. Following this same procedure with the low- T ($1\text{ mHz} < \nu_p < 10\text{ kHz}$) dielectric data leads to an extrapolation of $w^{-1}=0$ at $T=114\pm 9$ K, which does not correlate well with $T_0=141\pm 5$ K.

It is apparent from looking at Figs. 3 and 4 that there may be a correlation between the behavior of the peak position and width of these relaxations. This has been noticed before^{2,24,25} in the context of comparing a num-

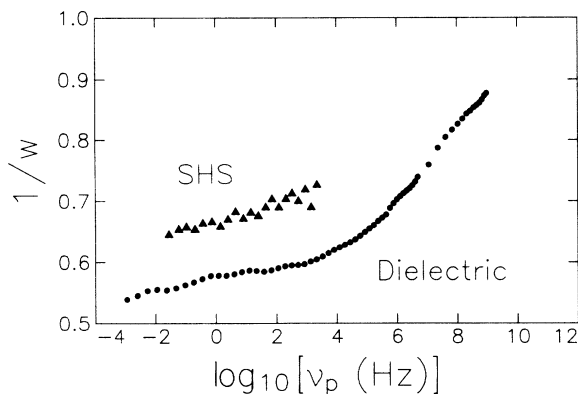


FIG. 5. Inverse width w^{-1} for SHS (Δ) and dielectric susceptibility (\circ) vs the peak position $\log_{10}[\nu_p$ (Hz)]. The dielectric susceptibility data show a clear change in slope in the frequency range where the measured T_0 values in Fig. 4 appear to stabilize. A continuation of the high-frequency trend in these data will lead to a normalized width of 1 in the neighborhood of $\nu_p \sim 10^{12}$ Hz; it appears as if the relaxation is tending toward a simple Debye form as the characteristic relaxation time approaches phonon frequencies.

ber of different susceptibilities of the glass transition that probe smaller nonoverlapping windows of the frequency range covered by this dielectric susceptibility measurement.¹⁵ The relationship between the peak position and width becomes more apparent when these data are plotted in a different fashion. In Fig. 5 we plot the inverse width w^{-1} versus the peak position $\log_{10}(\nu_p)$. These data show a clear change in slope in the frequency range where the measured T_0 values in Fig. 4 appear to stabilize; this suggests the possibility that the relaxation mechanism may be changing in this range. A continuation of the high-frequency trend in these data will lead to a normalized width of 1 at a frequency in the neighborhood of $\nu_p \sim 10^{12}$ Hz ($\omega_p = 2\pi\nu_p \sim 10^{13}$ rad/sec). In other words, it appears as if the relaxation is tending toward a simple Debye form as the characteristic relaxation time approaches phonon frequencies.

E. Static susceptibilities

Along with the dynamics information that we obtain with these techniques, we also obtain information about the static properties of the liquid, namely, the static susceptibilities. In Fig. 6(a) we plot the static susceptibilities $\Delta\epsilon = [\epsilon(\nu=0) - \epsilon(\nu=\infty)]$ and $\Delta c_p \kappa$ versus $1/T$. Both

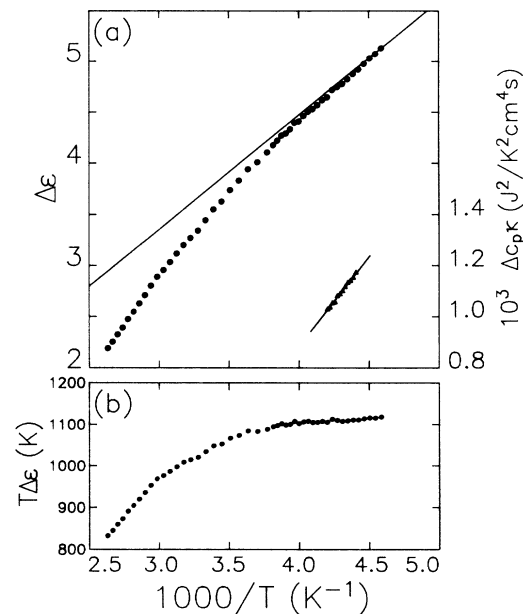


FIG. 6. (a) Static susceptibilities $\Delta\epsilon(\circ)$ and $\Delta c_p \kappa$ (Δ) vs $1000/T$ (K^{-1}). Both sets of data were obtained from the stretched-exponential fits to the data shown in Figs. 1 and 2. The SHS data points shown are the temperatures in the middle of the frequency window. These points were used to obtain the constraining form that is also shown: $\Delta c_p \kappa(T) = -1.93 \times 10^{-3} + 0.703/T$ ($\text{J}^2/\text{K}^2 \text{cm}^4 \text{s}$). The $\Delta\epsilon$ data in (a) are only constrained above 335 K and below 222 K. The curve in (a) is a Curie-law fit to the dielectric data below 225 K. (b) Product $T\Delta\epsilon$ (K) vs $1000/T$ (K^{-1}) for the dielectric susceptibility data. If the dipoles are uncorrelated over the entire range of the measurement, then $T\Delta\epsilon$ should be proportional to the density of the liquid.

sets of data were obtained from the stretched-exponential fits to the data shown in Fig. 1 and 2.

In the case of SHS, we started by performing three parameter stretched-exponential fits to the $c_p \kappa''$ data. These fits systematically deviate from the "full-peak" parameter values as the relaxation moves out of our frequency window. We corrected for this problem by fitting the $\Delta c_p \kappa(T)$ data in the middle of our window and using the form obtained to constrain the fitting to two parameters: ν_{SE} and β . The SHS data points shown in Fig. 6(a) are the points in the middle of the window that were used to obtain the fitting form $\Delta c_p \kappa(T) = -1.93 \times 10^{-3} + 0.703/T$ [$J^2/K^2 \text{ cm}^4 \text{ s}$], which is also shown.

Laughlin and Uhlmann⁴ have measured c_p for both the supercooled liquid and the crystal over this range. Since, in general, the difference in c_p between the crystal and glass is found to be negligibly small, we can divide our $\Delta c_p \kappa(T)$ data by their result [$\Delta c_p(T) = c_p(\text{liquid}) - c_p(\text{crystal}) = 2.14 - 6.26 \times 10^{-3} T$ ($J/\text{cm}^3 \text{ K}$)] to obtain $\kappa(T) \sim 0.0016$ ($J/\text{cm}^3 \text{ K s}$). It is essentially flat over this range, dropping less than 3%. Although SHS has an absolute accuracy of $\sim 25\%$, its relative accuracy [and hence the relative accuracy of this $\kappa(T)$ measurement] is $\sim 2\%$. We are unaware of any $\kappa(T)$ data for salol, but this result is consistent with expectations based upon data for similar organic liquids.²⁶ The relative magnitude of the static susceptibility through the relaxation $c_p \kappa(\nu = \infty)/c_p \kappa(\nu = 0) = 0.68$ at 240 K is found to agree within 3% with the ratio of the liquid and crystal values from Laughlin and Uhlmann:⁴ $c_p(\text{crystal})/c_p(\text{liquid}) = 0.66$ at 240 K. This is consistent with the proposition that κ plays no dynamic role in the glass transition as has been found previously.¹⁰ It has been demonstrated that molecular-dynamics simulations of the glass transition display frequency-dependent specific heat.¹³ Recent results from these simulations indicate that the thermal conductivity shows no dispersion in the glass transition;²⁷ this is in agreement with our measurements.

In the case of dielectric susceptibility, we have a very large bandwidth; this allowed us to perform three parameter fits to the data over most of the range. The $\Delta \epsilon$ data in Fig. 6(a) are only constrained above 335 K and below 222 K. In contrast to $\Delta c_p \kappa$, $\Delta \epsilon$ shows a very strong temperature dependence. For the case of independent dipoles, we would expect a simple Curie-law behavior of the static susceptibility: $\Delta \epsilon \propto 1/T$. The curve in Fig. 6(a) is a Curie-law fit to the data below 225 K. Obviously, it is a very poor fit to the data; $\Delta \epsilon$ is growing faster than $1/T$ over the entire range of the measurement.

Since our sample is a liquid and is free to flow in and out of the active regions of our measurement cells, we must take into account the fact that the number of dipoles we measure varies with the density of the liquid $\rho(T)$, i.e., $\Delta \epsilon \propto \rho(T)/T$. In Fig. 6(b), we plot the product $T \Delta \epsilon$ versus $1/T$. If the dipoles are uncorrelated over the entire range of the measurement, then we would expect $T \Delta \epsilon$ to be proportional to the density of the liquid. If we assume that this is true, then the thermal expansion coefficient $\alpha = -(\partial \rho / \partial T) / \rho$ that we obtain from these data varies from $\alpha(380 \text{ K}) = (1.9 \pm 0.2) \times 10^{-3}$ to $\alpha(220 \text{ K}) = (3 \pm 1) \times 10^{-4}$. Although α shows a surprisingly rap-

id change with temperature, these values are the right order of magnitude for an organic liquidlike salol in this temperature range.²⁶ The temperature dependence of the static quantity $T \Delta \epsilon$ appears to be correlated with the behavior of the relaxation. α changes rapidly in the same region where the peak relaxation frequency appears to break.

It is also possible that the dipoles are not behaving in an independent Curie-law fashion. This also may contribute to the deviation from Curie-law behavior. To determine if this is the case requires an independent measurement of the density over this temperature range; we hope to do this in the future.

F. Scaling of SHS data

It was recently determined that the dielectric susceptibility data for salol and a number of other organic glass formers can be scaled onto a single master curve that is the same for all of the liquids.¹⁵ The observation that all of the dielectric relaxation data that was obtained deviated from stretched-exponential behavior in a consistent fashion led the authors to ask whether all of these data could be scaled onto a single relaxation form. These efforts resulted in a scaling plot which satisfied this requirement and established that only two parameters, the width and peak position, are necessary to describe the dielectric relaxation data at each temperature.

We have plotted our salol SHS data in this fashion to determine if it also obeys this scaling relationship. In Fig. 7 we show the SHS data over our entire temperature range on such a scaling plot. The abscissa is $\omega^{-1}(1 + \omega^{-1}) \log_{10}(\nu/\nu_p)$. The ordinate is $\omega^{-1} \log_{10}[(c_p \kappa'')\nu_p / (\Delta c_p \kappa)\nu]$. The motivation for this scaling form is discussed in Ref. 15. This scaling leads to a satisfactory collapse of the data. The dashed line in the figure shows

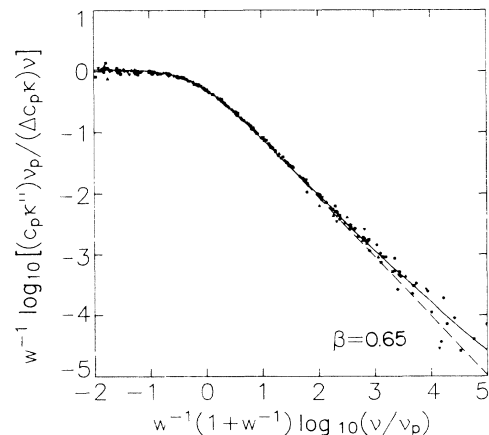


FIG. 7. Entire range of $c_p \kappa''$ data for salol scaled in the manner used to scale the dielectric data for salol and other liquids in Ref. 15. The abscissa is $\omega^{-1}(1 + \omega^{-1}) \log_{10}(\nu/\nu_p)$. The ordinate is $\omega^{-1} \log_{10}[(c_p \kappa'')\nu_p / (\Delta c_p \kappa)\nu]$. The dashed line is a stretched exponential form with $\beta = 0.65$ scaled in this manner. The solid line is the master scaling shape obtained from collapsing the dielectric data for salol and a number of other liquids.

what a stretched-exponential form with $\beta=0.65$ gives if plotted in this way; the solid line shows the scaling form obtained from the dielectric susceptibility data. Unfortunately, the SHS data are not accurate enough to determine whether or not it scales like the dielectric data or the stretched-exponential form. Planned improvements in the technique should allow us to resolve this in future measurements.

G. Peak relaxation frequencies, high T

Over the last 6 years, there has been significant development in the mode coupling theories of the glass transition.^{28–31} In general, these theories treat the slowing down in the liquid as a purely kinetic effect. Starting from a mode coupling mechanism in the simple liquid state (a feedback from the first Fourier component of the density correlation function to the viscosity), they obtain a power-law divergence of the viscosity η with decreasing temperature: $\eta = \eta_m (T/T_x - 1)^{-\alpha}$, where T_x is the divergence temperature and the exponent $\alpha = 1.8$. Other relaxation times should obey the same relationship. The more recent work^{30,31} indicates that higher-order terms cutoff the divergence at some point. Although these theories clearly fail in the high-viscosity regime, they appear to be successful in predicting the behavior of the viscosity of a number of fragile glass formers for $\eta < 10$ poise.³²

In Fig. 8 we test the mode-coupling-theory scaling prediction $\nu_p = \nu_m (T/T_x - 1)^{1.8}$ using the dielectric peak frequency data for salol. In Fig. 8(a) we plot $\nu_p^{1/1.8}$ versus

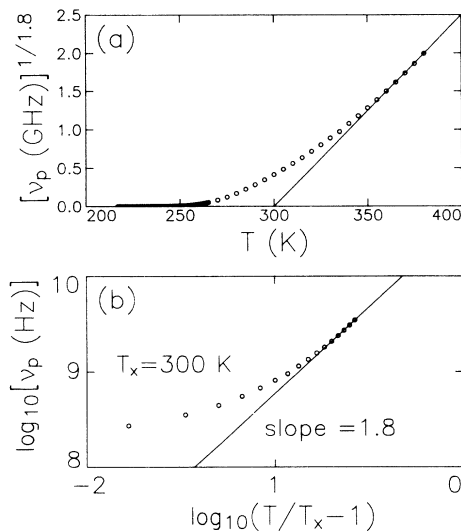


FIG. 8. Mode-coupling-theory scaling plots of the dielectric peak frequency data; the mode-coupling-theory prediction is $\nu_p = \nu_m (T/T_x - 1)^{1.8}$. (a) $[\nu_p \text{ (GHz)}]^{1/1.8}$ vs T (K). The curve is a linear fit to the last four points, which gives $T_x = 300$ K. (b) $\log_{10}[\nu_p \text{ (Hz)}]$ vs $\log_{10}(T/T_x - 1)$, where we use the value $T_x = 300$ K obtained from (a). The curve is a power law with an exponent 1.8. Clearly, the data in our frequency window do not obey this scaling relation with the possible exception of the data above 1 GHz.

T , which should show linear behavior if the data scale with an exponent $\alpha = 1.8$; the curve is a linear fit to the last four points, which gives $T_x = 300$ K. In Fig. 8(b) we plot $\log_{10}(\nu_p)$ versus $\log_{10}(T/T_x - 1)$, where we use the value $T_x = 300$ K obtained from Fig. 8(a). The curve in Fig. 8(b) is a power law of 1.8. Our data do not extend far enough above $\nu_p = 1$ GHz ($\eta \sim 10$ poise) to really test the scaling behavior. Clearly, the data in our frequency window do not obey this scaling relation with the possible exception of the data above 1 GHz. These data are consistent with the behavior observed in the low-viscosity regime of other fragile glass formers.³²

Mode coupling theory is clearly inapplicable for $\nu_p < 1$ GHz. The mechanism in mode coupling theory that relaxes local perturbations is viscous dissipation. In the entropic picture of the glass transition, local rearrangements of the molecules are seen as activated processes. In 1969, Goldstein³³ argued that the relaxation should start to take on an activated character for $\nu_p < 1$ GHz. Note that this is right where mode coupling theory breaks down. If this view is correct, then we can interpret the “elbow” region in Fig. 3(a) as the crossover between these two regimes.

IV. SUMMARY

In contrast to viscosity measurements of salol, our measurements show that the characteristic relaxation time measured by SHS and dielectric susceptibility is not Arrhenius near T_g . For $\nu_p < 10$ kHz we find that the peak relaxation frequency is diverging in a stable Vogel-Fulcher manner with $T_0 \approx T_K$. Our SHS and dielectric susceptibility measurements of the glass transition in a number of other liquids also behave in this fashion.^{6–8,10,11,15} This supports the view that the observed dynamic slowing down in the liquid is being driven by an underlying thermodynamic phase transition.

The peak relaxation frequencies obtained from these two techniques agree quite well; this is not the case for the relaxation widths. A comparison of SHS and dielectric width data for a number of different liquids^{11,15} has not clarified the relationship between these two widths. A simple empirical extrapolation of the SHS width indicates that it may be diverging in the neighborhood of T_K ; we also found this to be the case for the fragile liquid *o*-terphenyl.¹⁰ Applying this same extrapolation to the dielectric susceptibility data leads to a much lower divergence temperature. We find this to be true in general for our dielectric susceptibility measurements;¹⁵ this suggests that the extrapolation of our SHS width data may be fortuitous.

As more liquids are measured with SHS, we find that the relaxation widths that we obtain for these different liquids all agree within error.¹¹ This suggests that the SHS width may be an invariant of the glass transition. In contrast, it has been found that the width measured with dielectric susceptibility varies greatly from one liquid to another.¹⁵ Establishing that the SHS width is an invariant of the glass transition and determining the relation-

ship between the SHS and dielectric widths requires that we proceed to study as wide a variety of glass-forming liquids as possible. It is also clear that expanding the frequency range of SHS on the high side would help a great deal in answering these questions.

An interesting correlation shows up in the data. The width of the dielectric relaxation appears to be related to the rate of divergence of the peak relaxation frequency; this shows up clearly in Figs. 3–5. This behavior is apparent in the dielectric susceptibility data on other liquids as well.¹⁵ As yet, we do not have a good understanding of this; nor do we understand why the width and local divergence temperature appear to break at $\nu_p \sim 10$ kHz. We intend to broaden the scope of our SHS and

dielectric susceptibility measurements to other types of glass-forming liquids to try to answer these questions.

ACKNOWLEDGMENTS

I wish to thank R. Ernst, L. Wu, N. Birge, B. Ellmann, C. A. Angell, and J. Sethna for stimulating discussions. The high-frequency dielectric data were taken in collaboration with Bruce D. Williams and John P. Carini at Indiana University; I wish to thank them for their contributions. I would especially like to thank Sidney Nagel for his guidance, support, and good cheer over the past few years. This work was supported in part by the National Science Foundation under Grant No. DMR 88-02284.

*Present address: Exxon Research and Engineering Company, Route 22 East, Annandale, New Jersey 08801.

¹W. Kauzmann, *Chem. Rev.* **43**, 219 (1948).

²C. A. Angell, in *Proceedings of the Workshop on Relaxations in Complex Systems, Blacksburg, VA, 1983*, edited by K. L. Ngai and G. B. Wright (U.S. Office of Naval Research, Arlington, VA, 1984).

³G. Adams and J. H. Gibbs, *J. Chem. Phys.* **43**, 139 (1965).

⁴W. T. Laughlin and D. R. Uhlmann, *J. Phys. Chem.* **76**, 2317 (1972).

⁵G. S. Grest and M. H. Cohen, *Adv. Chem. Phys.* **48**, 455 (1981).

⁶N. O. Birge and S. R. Nagel, *Phys. Rev. Lett.* **54**, 2674 (1985).

⁷N. O. Birge, *Phys. Rev. B* **34**, 1631 (1986).

⁸N. O. Birge, Y. H. Jeong, and S. R. Nagel, *Ann. N.Y. Acad. Sci.* **484**, 101 (1986).

⁹N. O. Birge and S. R. Nagel, *Rev. Sci. Instrum.* **58**, 1464 (1987).

¹⁰P. K. Dixon and S. R. Nagel, *Phys. Rev. Lett.* **61**, 341 (1988).

¹¹P. K. Dixon and S. R. Nagel, in *Proceedings of the 18th North American Thermal Analysis Society Conference*, edited by I. R. Harrison (NATAS, University Park, PA, 1989), p. 290.

¹²D. W. Oxtoby, *J. Chem. Phys.* **85**, 1549 (1986).

¹³G. S. Grest and S. R. Nagel, *J. Phys. Chem.* **91**, 4916 (1987).

¹⁴T. Christensen, *J. Phys. (Paris) Colloq.* **46**, C8-635 (1985).

¹⁵P. K. Dixon, L. Wu, S. R. Nagel, B. D. Williams, and J. P. Carini, *Phys. Rev. Lett.* **65**, 1108 (1990).

¹⁶D. W. Davidson and R. H. Cole, *J. Chem. Phys.* **19**, 1484

(1951).

¹⁷V. Provenzano, L. P. Boesch, V. Volterra, C. T. Moynihan, and P. B. Macedo, *J. Am. Ceram. Soc.* **55**, 492 (1972).

¹⁸J. Wong and C. A. Angell, *Glass: Structure by Spectroscopy* (Dekker, New York, 1976), Chap. 11.

¹⁹P. K. Dixon and Lei Wu, *Rev. Sci. Instrum.* **60**, 3329 (1989).

²⁰C. T. Moynihan *et al.*, *Ann. N.Y. Acad. Sci.* **279**, 15 (1976).

²¹Hewlett-Packard, Product Note No. 8510-3 (Hewlett-Packard, P.O. Box 3640 Sunnyvale, CA 94088-3640).

²²R. O. Davies and J. Lamb, *Proc. Phys. Soc. London, Ser. B* **69**, 293 (1956).

²³C. E. Miller, *J. Cryst. Growth* **42**, 357 (1977).

²⁴K. L. Ngai, in *Non-Debye Relaxation in Condensed Matter, Proceedings of a Discussion Meeting, Bangalore*, edited by T. V. Ramakrishnan and M. Raj Lakshmi (World Scientific, Singapore, 1987).

²⁵S. R. Nagel and P. K. Dixon, *J. Chem. Phys.* **90**, 3885 (1989).

²⁶*Thermophysical Properties of Matter*, TPRC Data Series, edited by V. S. Touloukian (IFI Plenum, New York, 1970).

²⁷R. M. Ernst, G. S. Grest, and S. R. Nagel (unpublished).

²⁸E. Leutheusser, *Phys. Rev. A* **29**, 2765 (1984).

²⁹U. Bengtzelius, W. Goetze, and A. Sjolander, *J. Phys. Chem.* **17**, 5915 (1984).

³⁰S. P. Das and G. F. Mazenko, *Phys. Rev. A* **34**, 2265 (1986).

³¹S. P. Das and G. F. Mazenko, *Phys. Rev. A* **36**, 211 (1987).

³²C. A. Angell, *J. Phys. Chem. Solids* **49**, 863 (1988).

³³M. Goldstein, *J. Chem. Phys.* **51**, 3728 (1969).